

Initial stages of oxygen adsorption on Si(111). II. The molecular precursor

U. Höfer, P. Morgen,* and W. Wurth

Physik-Department (E20), Technische Universität München, D-8046 Garching bei München, Federal Republic of Germany

E. Umbach

Physikalisches Institut, Universität Stuttgart, Postfach 80 11 40, D-7000 Stuttgart 80, Federal Republic of Germany

(Received 8 November 1988; revised manuscript received 1 March 1989)

In the initial stage of oxygen adsorption on Si(111) surfaces, a metastable molecular state is found which precedes dissociation and insertion of oxygen atoms in bridging positions between first- and second-layer silicon atoms. This precursor can be observed in conventional photoemission experiments at low coverages and—for optimum retention—at low substrate temperatures. Combining the results from several high-resolution electron spectroscopies such as x-ray photoemission (XPS), polarization- and photon-energy-dependent uv photoemission, x-ray-induced Auger spectroscopy, and near-edge x-ray absorption, we are able to characterize the precursor as a negatively charged molecular species chemisorbed in a bridge configuration between dangling bonds of the surface. Its decay and conversion into the stable dissociated state could be monitored by XPS up to room temperature, showing a thermally or electronically activated behavior. For the reaction of O₂ with Si(111), a two-stage adsorption model is proposed. It explains a number of observations and features of oxygen adsorption on differently prepared Si(111) surfaces. The present model may be applicable to other semiconductor surfaces as well.

I. INTRODUCTION

The present paper is the second part of an extensive study of oxygen adsorption on differently prepared Si(111) surfaces at room and liquid-nitrogen temperatures. In part I,¹ we have concentrated on room-temperature adsorption. In agreement with other recent results obtained with improved experimental techniques²⁻⁶ a main conclusion was that at 300 K oxygen adsorption terminates dissociatively on Si surfaces. Even at the lowest coverages oxygen can break the backbonds between top and second Si layers and forms Si—O—Si bridge configurations similar to SiO₂. After years of controversial debate this common conclusion derived from studies using different spectroscopies represents a remarkable progress which also affects the detailed microscopic understanding of thin SiO₂ films and the Si/SiO₂ interface.⁷⁻⁹

From a more detailed point of view, however, the situation appears less clear. Generally we still have less insight into the mechanisms of adsorption and reaction on semiconductor surfaces than on metal surfaces. Considering the system O₂/Si, which can be regarded as a kind of prototype in this context, several phenomena occurring during the initial step of adsorption have yet to be understood. Important questions that remain unanswered, or are even brought up by the identification of adsorbed oxygen as an oxidelike state, are for example: What is the role of the dangling bonds? What is the reason for the influence of surface orientation and reconstruction on oxygen uptake? Are there any minority species and what is their electronic configuration? What is the reason for the striking change of the sticking coefficient near half-monolayer coverage? While coad-

sorption experiments,¹⁰ comparison of differently oriented and reconstructed surfaces,^{11,12} or adsorption and decomposition of other molecules such as NO (Ref. 13) or N₂O (Refs. 14 and 15) can help to answer these questions, we believe that the key is still a careful investigation of the first steps of the interaction of O₂ with a well-defined Si surface.

Most progress in this direction has probably been achieved for O₂ adsorption on the Si(111) surface, so far. In a previous article we have shown that the dissociative adsorption of oxygen on Si(111) is preceded by a metastable precursor.⁴ Our UPS data using polarized uv light indicated that the precursor is a molecularly chemisorbed oxygen species. Of two possible molecular configurations, the peroxy radical or the peroxy bridge, only the latter appeared to be in agreement with our results.⁴ The data presented in this paper are meant to complement and support our previous results.

The spectroscopies applied are high-resolution x-ray photoelectron spectroscopy (XPS), angle-resolved uv photoelectron spectroscopy (UPS) with polarized light including data taken with synchrotron radiation, high-resolution x-ray-induced Auger-electron spectroscopy (XAES), near-edge x-ray-absorption fine-structure (NEXAFS) spectroscopy, and work-function changes ($\Delta\Phi$). Our earlier results⁴ will be presented and discussed in more detail but also new evidence will be given for the characterization of the precursor. With respect to part I we concentrate on low oxygen coverages, low substrate temperatures, and the [7×7] reconstructed surface. These are the conditions under which the precursor can be observed best. Results obtained at room temperature and on differently prepared Si(111) surfaces are included as far as they are relevant for the discussion of the pre-

cursor.

Specific emphasis will be given to a profound characterization of the metastable state based on the results from various spectroscopies. Some controversy has been introduced into the present subject by the quoted results of other studies considering low substrate temperatures and/or low oxygen coverages. Ibach *et al.*² previously observed additional losses with EELS at low temperatures that were not present at higher substrate temperatures. Dissociated oxygen, double bonded in an on-top position, and a molecular peroxy radical were considered as possible interpretations for these losses. Whereas Ibach *et al.* were in favor of the latter model with arguments that can also be applied to a peroxy-bridge configuration, Schell-Sorokin and Demuth⁵ later came to a different conclusion. Based on electron-energy-loss spectroscopy (EELS) data, which confirmed those of Ibach *et al.*, in combination with UPS results, they excluded molecularly chemisorbed oxygen and suggested that the low-temperature species should be essentially a double-bonded SiO molecule adsorbed on the Si surface similar to CO on metals.

In a photoemission study using synchrotron radiation Hollinger *et al.*⁶ identified the shoulder seen in the O 1s core spectra at higher binding energy with this low-temperature species as the shoulder disappeared upon annealing to 500°C. Like Schell-Sorokin and Demuth they rejected any molecular species based on their UPS results. Furthermore they excluded oxidation models that involve different stages of adsorption by the observation that the relative intensity of the O 1s shoulder with respect to the main peak stays approximately constant through the whole adsorption range. This O 1s shoulder was also found in Ref. 11 but there two regions with different sticking coefficients were clearly distinguished in the uptake curve for oxygen on Si(111) below monolayer coverage. The present experiments on the precursor and its decay actually clarify this seeming contradiction and explain the varying quantities of minority species visible in previously reported data.^{3,16}

In the next section (II) we give a short description of the data-analysis procedures used in this paper and part I for enhancement and quantitative evaluation of our XPS data. In Sec. III XPS results are presented which demonstrate the existence of a metastable precursor and are used for a quantitative evaluation of its decay under different conditions. In Sec. IV the precursor is characterized as a molecular oxygen species mainly based on the present UPS data, and on $\Delta\Phi$, XAES, NEXAFS, and high-resolution electron-energy-loss spectroscopy (HREELS) results some of which are discussed in more detail elsewhere. In Sec. V we show the influence of different surface preparations and of oxygen coverage on the precursor and propose a model for the initial stage of oxygen adsorption on silicon including the molecular precursor. Finally, a short summary is given in Sec. VI.

II. EXPERIMENTAL METHODS

A. General remarks

Experimental facilities and sample preparation are described in detail in part I and will not be repeated here.

However as the measurements reported below involve different substrate temperatures a few words on the temperature control appear appropriate. Our system is equipped with a sample exchange mechanism. The movable sample holder consists of a small copper block that fits into a larger block mounted on a rotatable manipulator. The silicon crystal was held by two tungsten wires fixed in the small Cu block, with a chromel-alumel thermocouple spot-welded to one of them. To prevent the formation of nickel silicide upon heating the sample, the thermocouple was not in direct thermal contact with the silicon sample. Thus the precision of temperature measurement was limited and is estimated to be $\pm 10\%$ of the temperature difference relative to room temperature.

A movable filament separately mounted on the manipulator flange was used for heating. Temperatures up to 500 K could be achieved by using heat radiation, higher temperatures by electron bombardment from the filament located behind the crystal with a positive bias applied to the sample. Cooling down to 120 K was initially provided by a liquid-nitrogen bath in thermal contact with the copper blocks. Later a helium cryostat allowed a minimum sample temperature of approximately 40 K.

B. Data analysis by Fourier smoothing and deconvolution

Some numerical procedures have been developed and applied to the data presented here. In particular, "optimal Fourier filtering" was used for smoothing spectra, and, in the case of XPS, instrumental broadening was deconvoluted by an iterative technique. The underlying principles will be outlined below; specific details are described elsewhere.¹⁷

The smoothing procedure uses the concept of optimal Wiener filtering of the Fourier-transformed (FT) data, which is well known in digital signal processing.¹⁸ If $\hat{s}(E) = s(E) + n(E)$ describes the measured data consisting of the true (uncorrupted) signal $s(E)$ and the noise $n(E)$, the Wiener filter is defined by

$$G(f) = \frac{|S(f)|^2}{|S(f)|^2 + |N(f)|^2}, \quad (1)$$

where $S(f)$ and $N(f)$ are the FT of $s(E)$ and $n(E)$, respectively. $G(f)$ is applied in Fourier space: $\bar{S}(f) = G(f)\hat{S}(f)$, and $\bar{s}(E) = \text{FT}^{-1}\{\bar{S}(f)\}$ is the smoothed result. It can be shown that $G(f)$ is optimum in the sense that the mean value of $\int dE |\bar{s}(E) - s(E)|^2$ is minimum.^{17,18}

The practical problem in constructing $G(f)$ is that only the corrupted signal \hat{s} , but not the constituents s and n , are known. This can be overcome by using specific features of the data for an approximation, especially taking into account the rather clear separation of signal and noise in a wide range of frequencies.^{17,19,20} Our algorithm divides the frequency space into four regions, wherein different approximations are made. This can be done automatically by a computer program and does not require any input parameters from the user.¹⁷ Whereas simpler schemes¹⁹ work sufficiently well for most data, they occasionally lead to oversmoothing of complicated structures. Our algorithm has proven to work reliably on

very different kinds of data from various surface techniques such as XPS, UPS, NEXAFS, energy-loss spectroscopy (ELS), temperature-programmed desorption (TPD), low-energy electron diffraction (LEED), etc. It has further been applied successfully to analyze two-dimensional spectra.²¹

Besides noise instrumental broadening leads to a corruption of the data. To a good approximation this effect can be described by a convolution of the physical data $f(E)$ with an instrumental function $h(E)$ resulting in the measured function

$$s(E) = \int dE' f(E') h(E - E'),$$

or $s = f \otimes h$, neglecting noise. Like data smoothing, deconvolution can be done in a straightforward way in Fourier space

$$f = \text{FT}^{-1}[\text{FT}(f)/\text{FT}(h)].$$

For reasons briefly discussed below we prefer an iterative approach. The algorithm is

$$f^{(k+1)} = f^{(k)} + \kappa(s - f^{(k)} \otimes h) \quad (2)$$

with $f^{(k)}$ being the result of the k th iteration and $f^{(0)} = s$. This is the well-known van Cittert method,²² except for the factor κ which was introduced by Jansson *et al.*²³ The relaxation factor $\kappa = \kappa(E, f^{(k)}(E))$ generally depends on the result of the last iteration $f^{(k)}$ and may be used to constrain the result of each iteration to physically meaningful values. For electron spectroscopic data we choose a function for κ which makes sure that $f^{(k+1)}(E)$ is positive for all E [$\kappa = 1$ if $f^{(k)}(E) \gg 0$; $\kappa \rightarrow 0$ if $f^{(k)}(E) \rightarrow 0$].¹⁷

The introduction of such constraints is rather important for deconvolution procedures in general and makes the resulting nonlinear methods superior to linear methods such as division in Fourier space or the simple van Cittert algorithm.²⁴ The latter methods usually lead to spurious oscillations in the result which are often hard to distinguish from real peaks. Compared to other more elaborate methods such as the maximum-entropy method^{24,25} the Jansson-van Cittert method has the advantage of being applicable to data of moderate signal-to-noise ratios, especially in combination with the described smoothing procedure.

Finally we like to comment on the spin-orbit decomposition used in part I for the Si $2p_{3/2}, 2p_{1/2}$ doublet. No deconvolution algorithm such as the Jansson-van Cittert method is needed in this case. The $2p_{1/2}$ component can simply be removed by the application of

$$f(E) = s(E) - r f(E + \Delta), \quad (3)$$

where r is the intensity ratio of $2p_{1/2}/2p_{3/2}$ (0.5) and Δ the doublet splitting [0.608 eV (Ref. 26)]. We assume identical line shapes for both components.³

III. DECAY OF THE PRECURSOR MONITORED BY XPS

A. Results at 150 and 300 K

The existence of a metastable precursor and its subsequent decay are most clearly demonstrated by the O 1s

core spectra taken at low coverage and low substrate temperature. Results obtained from a $[7 \times 7]$ -reconstructed Si surface exposed to 2.5 L [1 Langmuir ($L \equiv 10^{-6}$ Torr sec)] oxygen at a surface temperature of 150 K are displayed in Fig. 1. From the bottom to the top of the left-hand side a series of five original spectra are shown which were recorded at different times t after dosing. In the spectrum taken immediately after adsorption ($t = 0$; bottom), a major peak at 531.6 eV and a shoulder at 530.5 eV binding energy can clearly be distinguished. This shoulder decreases with time and disappears completely after sufficiently long elapsed time ($\approx 2h$, not shown) or after annealing. The spectrum of a layer obtained after annealing at about 400 K for 5 min is shown at the top of Fig. 1. Here the better statistics is due to a prolonged recording time of 30 min, compared to 5 min, at otherwise identical conditions.

On the right-hand side of Fig. 1 we present results obtained after deconvolution of the instrumental function by the technique described in Sec. II. They more clearly show the existence of a second adsorbate state, the metastable precursor, represented by a peak at 1.1 eV lower binding energy than the main peak. The contribution of the precursor to the total oxygen coverage (30% shortly after dosing) can be determined from these spectra by simple decomposition. The deconvolution reveals that

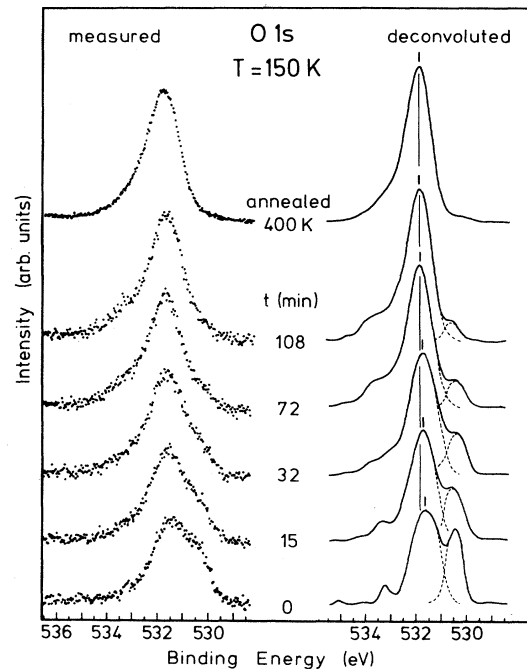


FIG. 1. Mg $K\alpha$ O 1s core-level spectra of Si(111)- $[7 \times 7]$ exposed to 2.5 L O_2 at 150 K. Recording of the lower five spectra on the left-hand side was started t minutes after adsorption; recording time was 5 min, and the overall resolution 0.76 eV. The topmost spectrum was obtained after mild annealing (recording time 30 min). The spectra on the right-hand side are the result of deconvolution of the instrument function. The spectra demonstrate the decay and conversion of the precursor (peak at 530.5 eV binding energy, referred to E_F) into the stable state (main peak at 531.6 eV).

the oxygen peak from the precursor is considerably narrower than the main O 1s peak of the stable state. As discussed in part I, in the stable state oxygen is dissociated and forms Si—O—Si bridges between the first two Si layers. Slightly different bond lengths and angles can give rise to different O 1s binding energies leading to a broader peak and may also be responsible for the weak structure around 533 eV binding energy.¹

Before we discuss the quantitative evaluation of the precursor decay we show results obtained at room temperature under otherwise identical conditions as for 150 K. Figure 2 displays the spectra recorded immediately after dosing and 6.5 or 20 min later. In contrast to the situation at 150 K the precursor is hard to detect in the untreated data. In the first spectrum at $t=0$ it contributes only about 20% to the total intensity, and after 20 min it has decayed to 5% under the influence of the (enhanced) substrate temperature. This short lifetime of the precursor has most likely prevented its identification in other recent photoemission work using O 1s core spectra.^{6,11} Only by using a position-sensitive detector to increase the analyzer sensitivity it was possible to achieve short enough recording times at the required resolution. The deconvolution technique helped to detect the weak features at room temperature.

B. Activation energy

The results of a quantitative evaluation of the precursor decay under different conditions are collected in Fig. 3. The relative precursor intensity referred to the total oxygen signal is displayed in a semilogarithmic plot versus time. Within the experimental accuracy all data points belonging to equivalent conditions lie on straight lines thus indicating exponential decay of the precursor. The precursor decays much more rapidly at room temperature than at 150 K. After a 2.5 L dose the lifetime τ ($1/e$ decay) is 14 min at 300 K (solid circles) and 60 min at 150 K. The x-ray source was switched on throughout the measurements in these cases. Without x-ray irradiation

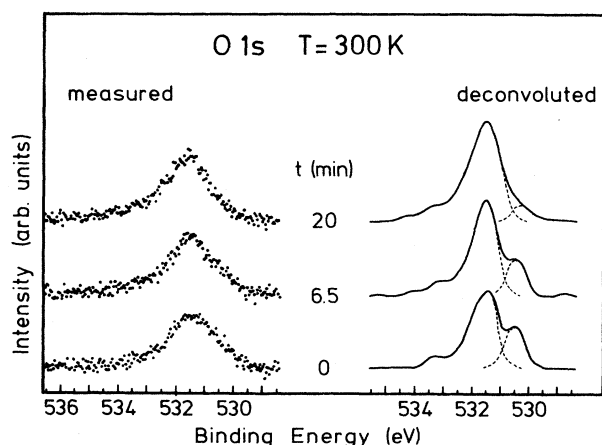


FIG. 2. Original (left) and deconvoluted (right) O 1s spectra of Si(111)-[7×7] exposed to 2.5 L O₂ at room temperature. Recording was started t minutes after adsorption.

the decay process is markedly retarded as indicated by dotted lines in Fig. 3. This result shows that, besides thermal activation, electronic processes can stimulate the dissociation reaction.

Within the simplest possible model the observed behavior of the precursor coverage θ can be described by a first-order reaction rate equation

$$R = -d\theta/dt = \theta[k_0 \exp(-E/k_B T) + k_e], \quad (4)$$

where the decay rate R of the precursor is proportional to the sum of two independent constants $k_T = k_0 \exp(-E/k_B T)$ and k_e , describing the influence of temperature and electronic excitation, respectively. The data indicate a negligible ($k < 0.1 \times 10^{-3} \text{ s}^{-1}$) thermal activation at 150 K, and hence we can set $k_e = (0.25 \pm 0.1) \times 10^{-3} \text{ s}^{-1}$ and $k_T(300 \text{ K}) = (0.95 \pm 0.2) \times 10^{-3} \text{ s}^{-1}$. An estimate for the activation energy E and the preexponential k_0 in k_T can be given taking into account the data obtained after annealing. Annealing at 400 K for 240 sec resulted in a 90% decrease of the precursor, i.e., $k_T(400 \text{ K}) = (10.0 \pm 3.0) \times 10^{-3} \text{ s}^{-1}$. This leads to $k_0 = 10 \text{ s}^{-1}$ and $E = 0.24 \text{ eV}$. A graphical plot of these values is shown in the inset of Fig. 3. Although this is a very rough estimate based only on three k_T values, the numbers give an idea of the kinetics of the precursor decay. Unfortunately it was impossible with our experimental setup to heat the crystal during the XPS measurements and thus to monitor the decay at temperatures other than 150 and 300 K.

Very recently Silvestre and Shayegan²⁷ derived an activation energy for the precursor decay of the same system monitoring work-function changes. However, their result, $0.045 \pm 0.015 \text{ eV}$, is not compatible with our value. Even if we allow for an unreasonably high error in our temperature control ($\pm 50 \text{ K}$ at 150 K and at 400 K) and

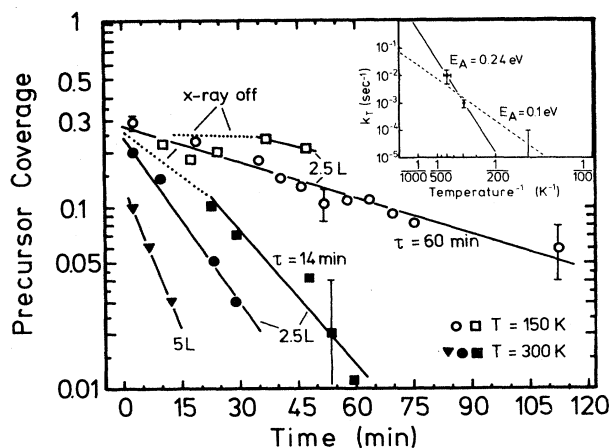


FIG. 3. Semilogarithmic plot of relative precursor intensity (referred to total oxygen coverage) vs time at 150 and 300 K substrate temperature, and for two different exposures. Dotted lines indicate intervals with the x-ray source turned off. $\tau = 1/(k_T + k_e)$ is the lifetime of the precursor, resulting from electronic and thermal activation [Eq. (4)]. The inset shows an estimate of the thermal activation energy; details are explained in the text.

in the quantitative evaluation of the relative precursor coverage (twice the error indicated in Fig. 3), our data exclude activation energies below 0.1 eV. This limit is shown in the inset of Fig. 3 by a dashed line. (The error bars in the inset give the mentioned enlarged limits.) We suppose that the reason for this discrepancy is a dependence of the decay rate upon oxygen coverage and especially on the amount of coadsorbed stable oxygen, which is not included in Eq. (4). Further discussion will be postponed until the results of different coverages have been presented in Sec. V A.

C. Different activation mechanisms

The decay of the precursor is not only activated by thermal motion or by x rays but also by high-flux electron bombardment (Fig. 4). However, low-energy photons such as those from a He discharge lamp did not have a detectable influence, even at a photon flux of about $10^{13} \text{ cm}^{-2} \text{ sec}^{-1}$ for He I, which is rather high compared to the flux from a Mg $K\alpha$ source ($\approx 10^{11} \text{ cm}^{-2} \text{ sec}^{-1}$).²⁸ Moreover the cross sections for core ionization excited with standard x-ray sources are usually smaller than those for valence levels excited with standard uv sources. Thus the data seem to indicate that a core hole is very efficient for dissociation.

A steep increase of the desorption rate is often seen in photon-stimulated desorption experiments if core thresholds of adsorbates are reached.²⁹ Thus our results suggest that the interpretation given there²⁹ is also applicable to the dissociation of the precursor. The decay of the core hole predominantly takes place by Auger transitions and thus leads to a double hole in the final state, in contrast to

the situation after primary ionization of a valence level (one hole). In the latter case the chemisorption bond enables an effective redistribution of charge and an immediate delocalization of the excitation into the bulk, but in the former case, the two holes can be strongly localized, due to Coulomb interaction, thus breaking the bond.²⁹

This interpretation applied to our example has one major drawback. The calculated cross sections for core-hole excitations are too small by 3–4 orders of magnitude. Hence additional or alternative mechanisms must play an important role. We suggest that secondary (e.g., Auger or photo-) electrons with sufficient energy ($> 100 \text{ eV}$) as well as collective excitations, such as plasmons, excitons, or phonons, initiated by core ionization and Auger decay, may play a major role for the decay of the precursor.

Another interesting finding in view of the precursor decay and activation mechanism is presented in Fig. 4, which compares O 1s spectra obtained after various treatments of a mixed adsorbate layer on Si(111) (2.5 L O_2 at 150 K ; spectrum at bottom). The different treatments were annealing at 400 K for 5 min , Mg $K\alpha$ exposure at 240 W for 150 min , and electron bombardment with 2 keV electrons (total dose 10^{18} electrons). In all cases the weak shoulder at the high-binding-energy side of the main O 1s peak is more pronounced after the decay of the precursor. It is weakest if the decay is activated by annealing and strongest if the decay is induced by electron bombardment. The rather broad and weakly structured shoulder obtained after x-ray irradiation can be reduced by additional heating to a shape and size similar to that obtained only by annealing. The spectrum measured after electron bombardment is not affected by such mild annealing. The latter spectrum had to be shifted by 0.3 eV to lower binding energy to align the main peak. We suppose that the whole surface is affected by electron bombardment.

The spectra shown in Fig. 4 demonstrate that the shoulder discussed by Hollinger *et al.* in Ref. 6 is due to a product of the decay of the precursor as is the main O 1s peak. The different spectra obtained after annealing and x-ray and electron irradiation are in support of our suggestion made in part I (Ref. 1) that the shoulder is not due to a completely different oxygen species, e.g., adsorbed in an on-top position, but that it is more likely the result of distorted Si—O—Si bridges. A rearrangement of adsorbate bonds should then be possible by annealing leading to a more homogeneous distribution in the adsorbate layer and hence to a sharpening of the O 1s peak, in agreement with the results. Mild annealing to $400\text{--}500 \text{ K}$, as employed here, leads to a diminishing of the intensity of the shoulder, whereas annealing at higher temperatures causes its complete disappearance.⁶

D. O 1s binding energies

Before concluding this section on the XPS results we should discuss the observed O 1s binding energies. Generally XPS core-level shifts (chemical shifts) are caused by changes of the partial charge in the ground state and by differences in relaxation (or screening) of the final state upon ionization. The latter effect can be viewed as being separable into intra-atomic (or intramolecular) relaxation

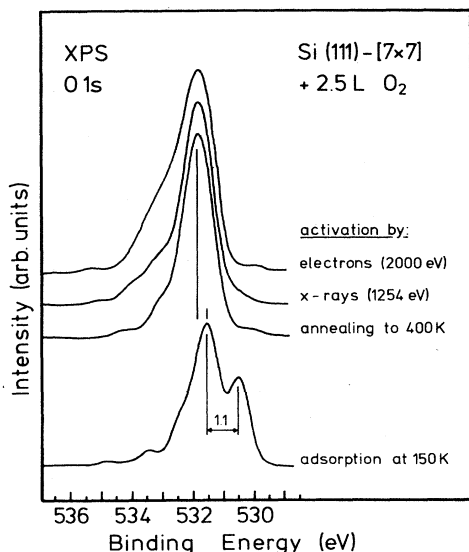


FIG. 4. Deconvoluted O 1s spectra of Si(111)-[7×7] exposed to 2.5 L O_2 at 150 K immediately after dosing (bottom) and after decay of the precursor activated by electron bombardment (total dose $3 \times 10^{18} \text{ electrons/cm}^2$), x-ray irradiation (240 W , 150 min), and annealing at 400 K (5 min). The top spectrum is shifted by 0.3 eV to lower binding energy in order to align the main O 1s peaks.

and external screening of the hole, for instance, by charge transfer from the surrounding solid. Both effects, additional negative charge density around the core electron, and improved screening of the final-state hole may lead to a lowering of the measured O 1s binding energy.

In the present case we observe three different O 1s features: the main peak at 531.6 eV representing the stable dissociated (majority) state, the shoulder at higher binding energies, and the new peak at 530.5 eV representing the metastable precursor state. The binding energy of the main peak is rather high for a dissociated oxygen adsorbate in the monolayer regime if we compare it to the binding energies found for atomic oxygen adsorbates on metal surfaces (~ 530 eV). Reduced screening and less negative charge on the oxygen adsorbate on Si are likely the reason for this shift. The latter argument is supported by recent NEXAFS results and theoretical considerations which lead to the conclusion that the partial charge on oxygen adsorbates is much smaller than that on the respective oxides.³⁰ The conclusion here is that the ionicity of oxygen on Si is particularly small ($\leq 50\%$).

The shoulder at higher binding energies (see, e.g., Fig. 4) is most likely *not* due to a different stable (minority) species as discussed above and in Ref. 1. Both alternative interpretations for this shoulder given in Ref. 1, as a satellite to the main peak or as representative for strained Si—O—Si bonds, are clearly compatible with the observed higher binding energy. For instance, distorted bonds should be accompanied by less charge transfer from the Si atoms to the oxygen and by less efficient screening of the final-state O 1s hole.

The low binding energy of the new peak at 530.5 eV representing the metastable precursor is easy to understand within the same picture if we refer to the results presented below. These results unambiguously show that the precursor is a molecular adsorbate state in a peroxy-bridge configuration which can be described as a negatively charged superoxo (O_2^-) species. The partial charge on this molecular O_2 adsorbate ($\sim 1e^-$), which is relatively high for adsorbed small molecules, is responsible for the enormous work-function change discussed below as well as for the observed O 1s binding energy, which is relatively low for molecular adsorbates. Hence the smaller binding energy of the molecular state as compared to the atomic adsorbate can be attributed to its higher negative charge. Efficient intramolecular relaxation in addition to charge-transfer screening from the Si neighbors may also contribute to this low binding energy. It is emphasized that the O 1s binding energies of equivalent molecular peroxy (or superoxo) species on transition-metal surfaces are in the same range [Pt(111), 530.6 (Ref. 31) and 530.8 (Ref. 32); Ag(110), 529.8 (Ref. 33)].

IV. CHARACTERIZATION OF THE PRECURSOR

Various spectroscopies have been used for characterization of the precursor. In this section we primarily report on UPS, $\Delta\Phi$, and additional XPS results, but also include the results from a recent synchrotron study of the precursor utilizing UPS, XAES, and NEXAFS (Ref. 34) and discuss HREELS results of two other groups.^{2,5} All

data corroborate our earlier suggestion of the precursor being a molecular oxygen species. We show that its molecular axis is oriented parallel to the surface and conclude that the precursor is a peroxylike species bridge bonded to the dangling bonds of two top-layer Si atoms.

A. UPS results

Figure 5 shows UP spectra taken with polarized uv light (21.2 eV; He I). The spectra in the middle represent a mixed layer of precursor and stable state, those at the top the stable state only; the spectra of a clean $[7\times 7]$ surface are plotted at the bottom. The comparison of top and bottom spectra shows that the structures labeled 7–9 are due to the stable state. Their energy position and polarization dependence is in support of atomic oxygen in the stable state forming a short bridge between two Si atoms in the first and second layer, as discussed in detail in part I.¹ (See also part I for a table of the energy positions of all labeled peaks.)

While the major part of the Si-derived valence band between 0 and 6 eV is only little affected by the stable species, the presence of the precursor results in two new prominent peaks (labeled 3 and 5) in this energy region at 2.1 and 3.9 eV, respectively. At higher binding energies only a rather weak structure labeled 6 may be attributed to the precursor. As already shown in Ref. 4, the intensities of peaks 3 and 5 are very different with He II light; peak 5 is very intense at this photon energy (40.8 eV) while peak 3 is almost undetectable.

A systematic investigation of the photon energy dependence has been performed with synchrotron radiation.³⁴ Selected spectra are collected in Fig. 6. Spectra 6(a)–6(e)

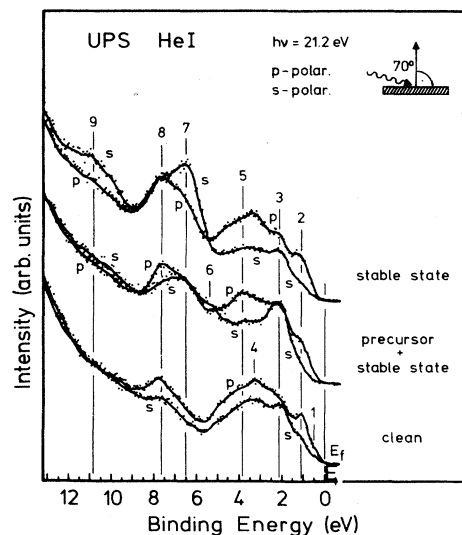


FIG. 5. Polarization (*s* and *p*) -dependent UPS spectra of a clean and two oxygen-exposed Si(111)- $[7\times 7]$ surfaces. Adsorbate preparation for the middle spectra (precursor and stable state) was the same as for the bottom spectrum of Fig. 1; the top spectra (stable state, only) correspond to the top spectrum of Fig. 1 and were obtained after annealing at 400 K. Prominent peaks and shoulders are labeled by numbers and are discussed in the text. Dots indicate measured data points, lines are the result of Fourier smoothing.

correspond to mixed layers of precursor and stable dissociated state, 6(g) represents a clean Si surface, and 6(f) a surface covered only with stable dissociated oxygen. The spectra show, for instance, a rapid decrease of the intensity of peak 3 with increasing photon energy and a resonant behavior of peak 5 around 38 eV, which is due to a σ shape resonance.³⁴ For a quantitative evaluation and discussion of the resonant behavior of peak 5 as a function of photon energy and for details concerning the experimental setup at the synchrotron source see Ref. 34.

To complete the UPS results we show in Fig. 7 the dependence of peaks 3 and 5 upon emission angle around the surface normal for *s*- and *p*-polarized He I light. The angular variation was achieved by rotation of the crystal with fixed uv source and *E* vector. Therefore the intensity variation does not exclusively reflect the dependence on emission angle but also includes that on slightly different polarizations of the incident light. Figure 7 shows that peak 3 is rather sharply directed towards the surface normal while there is no significant change of peak 5 with *p*-polarized light.

An assignment of the UPS structures to levels of the proposed adsorbate configuration will be given below, after the results from other spectroscopies have been presented. Here we only point out that the UPS data clearly indicate that the precursor is a molecular oxygen

adsorbate, for the following reasons. The two main peaks at 2.1 and 3.9 eV are in an energy region where no peaks from dissociated oxygen have been found but are expected for peroxy adsorbates from theoretical calculations.³⁵⁻³⁸ The resonant behavior of peak 5 is typical for molecules or molecular adsorbates indicating a transition from a σ state into a σ shape resonance. We also emphasize that the strong dependence of peak 5 on photon energy, and the energy and angular dependence of peak 3 are further reasons why the precursor species has not been identified in earlier photoemission work.^{3,5,11,16}

B. Work-function changes

Our He I spectra were recorded with a -15 V bias applied to the crystal. This bias allowed us to measure the low-energy cutoff of the secondary electrons which is determined by the work function of the sample. The work function Φ was found to be 4.4 eV for the clean Si(111) surface and $\Phi=4.60-4.65$ eV for an oxygen-covered surface, with oxygen only in the stable dissociated state. The latter value was almost constant up to a coverage of 0.5 ML. In contrast, layers containing the precursor yielded much higher work-function values. Figure 8 displays the observed work-function changes $\Delta\Phi$ with increasing coverage compared to the clean surface. The work function increases from $\Phi=4.4$ to 5.05 eV if the coverage of the precursor is increased to the maximum value of ≈ 0.1 ML. The $\Delta\Phi$ value of 0.65 eV is extraordinarily high, in view of such a low absolute

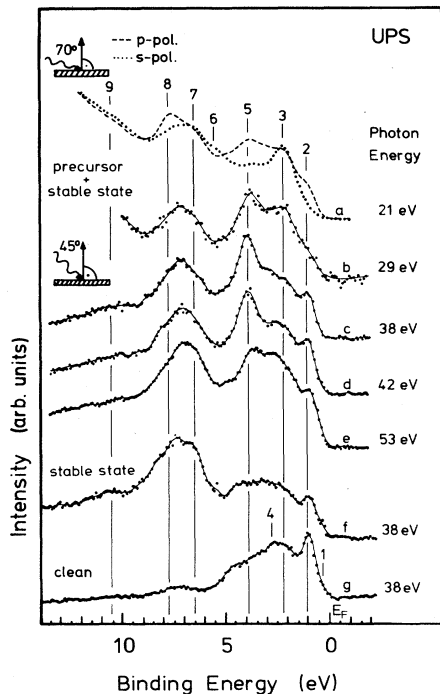


FIG. 6. UP spectra of mixed layers of precursor and stable state at various photon energies (a)–(e) are compared to spectra of an annealed layer (f), stable dissociated oxygen only, and of a clean surface (g). Measurement geometries as indicated. The top spectra of different polarization [(a) 21.2 eV] are taken from Fig. 5. The other spectra were recorded with the *E* vector lying in the plane of incidence (*p* polarization) and are taken from Ref. 34.

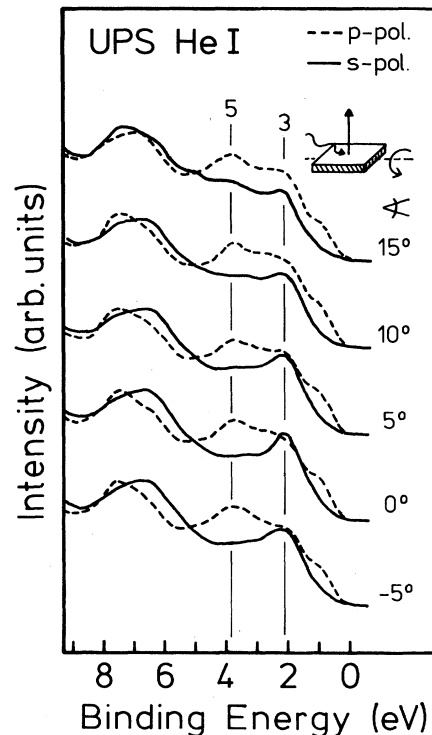


FIG. 7. Angular dependence of the prominent UPS structures of the precursor (in a mixed layer) around surface normal (0°).

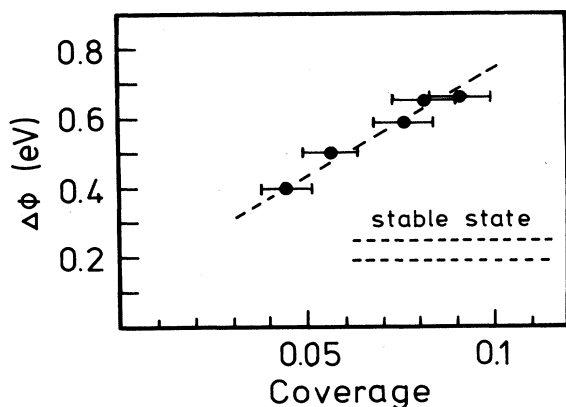


FIG. 8. Work-function changes $\Delta\Phi$ of layers containing the precursor for different precursor coverages (referred to Si surface atoms, $1.12 \times 10^{15} \text{ cm}^{-2}$). The work-function change of the surface covered only with the stable state lies between the dashed lines for all coverages from ≈ 0.1 up to a monolayer.

coverage of the precursor. To explain this observation a very strong dipole field is necessary which can only be understood if oxygen is adsorbed above the silicon surface and if considerable charge transfer to the oxygen molecule has occurred.

Based on $\Delta\Phi$ experiments, Silvestre and Shayegan derived an activation energy of the precursor,²⁷ as mentioned above. Their reported work-function changes ($\Delta\Phi_{\text{max}} = 1.6 \text{ eV}$) are even higher than ours, a result that we attribute to higher precursor coverages obtained at substrate temperatures below 20 K and/or perhaps to the different measurement technique. As we observe an almost linear increase of the work function with coverage (the latter independently derived from the O 1s signal), we confirm the assumption of Ref. 27 that $\Delta\Phi$ is proportional to the coverage, at least in the low-coverage regime.

C. Si 2p and O 2s levels

Spectra of the Si 2p core levels and of the 2s levels of oxygen have been recorded for mixed layers of precursor and stable state and have been compared to spectra from annealed layers. Though the results do not give significant new arguments for the characterization of the precursor, they are reported here for the sake of completeness.

After oxygen adsorption the Si 2p levels generally show weak satellite structures whose origin is discussed in part I.¹ Conversion of the precursor species into the stable state leads to an increase of the structures between 1.8 and 3.5 eV whereas the satellite at 0.9 eV below the main Si 2p_{3/2} component remains unchanged. This result is in agreement with the suggested configurations for stable state and precursor. Regardless of the exact origin (losses or chemical shifts) of the Si 2p satellite structures we expect less intensity in the case of an on-top bound (molecular) adsorbate than for atomic oxygen in bridge position between two silicon atoms, in agreement with experimental results.

The oxygen 2s levels have been investigated since they are split by about 14 eV into bonding ($2\sigma_g$) and antibonding ($2\sigma_u$) states in the case of the isolated O₂ molecule,³⁹ and since it seems possible to compare them to theoretical predictions. For instance, calculations for O₂ on Si(111) from Chen *et al.*³⁶ (peroxy radical) predict split O 2s levels while those of Kunjunny and Ferry³⁷ on Si(100) (peroxy bridge) do not. Unfortunately, we observed only slight changes in the spectra before and after annealing and could not resolve discernible peaks in the presence of the precursor. Even the identification of the O 2s level of the stable (atomic) oxygen state turned out to be difficult at low coverages using synchrotron radiation because of its broad structure and because it interferes with plasmon losses of silicon valence-band electrons.

This negative result is not unexpected. Cederbaum and coworkers⁴⁰ have shown that photoionization of inner valence levels of molecules is governed by strong correlation effects leading to a splitting of the photoemission signal into many final states of similar (and hence weak) intensity spread over an energy range of several eV. Thus we expect only a very broad and weak O 2s-derived signal from the molecular precursor which is unlikely to be discernible from background noise as well as from plasmon losses and O 2s structures of the coadsorbed stable state. Hence the missing intensity from the precursor is in accordance with, but of course no proof for, its molecular nature. Likewise only a very broad structure due to an O 2s-derived orbital has been observed for molecular O₂ on Pt(111).³²

D. XAES, NEXAFS, and HREELS results

Synchrotron radiation was used in a very recent study to provide complementary data for the characterization of the precursor.³⁴ In particular NEXAFS near the O 1s edge and XAES measurements were applied. For XAES the primary core hole cannot be excited by a conventional Al K α laboratory source or even by electrons because of the sensitivity of the precursor to high-energy electrons and photons, as discussed in Sec. III. Only excitation by synchrotron radiation near the O 1s threshold provides maximum intensity and minimum background for short enough recording times.

In part I,¹ we have compared oxygen KLL Auger spectra of isolated O₂, stable dissociated O/Si(111), SiO₂, and O/W(110). The similarity between the Auger line shapes of adsorbed oxygen on silicon with those of SiO₂ indicates that the local electronic character of the oxygen-derived orbitals is similar for adsorbed oxygen and for SiO₂.¹ In contrast, the Auger spectra of layers containing the precursor are markedly different.³⁴ They show additional fine structure which is related to corresponding Auger transitions found in the spectra of isolated O₂. This is another clear indication for the molecular nature of the precursor. Moreover, the very weak signal in normal emission from Auger transitions leading to a $4\sigma 4\sigma$ double-hole final state is in support of an orientation of the adsorbed molecule parallel to the surface.³⁴

The NEXAFS spectra monitored with O Auger partial yield show two additional structures for layers containing

the precursor compared to those containing only the stable dissociated state. Their polarization dependence unambiguously relates these peaks to π and σ resonances of an oxygen molecule with its axis parallel to the surface as reported in detail in Ref. 34. From the position of the σ shape resonance an O-O distance of about 1.28 Å can be derived.³⁴

HREEL spectroscopy was used by Ibach *et al.*² and Schell-Sorokin and Demuth⁵ for the investigation of oxygen adsorbed on silicon at different substrate temperatures. Besides losses due to bridge-bonded dissociated oxygen both groups found additional losses (the most intense at 1230 cm^{-1} = 152 meV) at low substrate temperatures. We identify these losses as arising from the precursor for the following reasons: The additional loss at 1230 cm^{-1} is weaker at room temperature than at ~ 100 K and was not found above 450 K. Its relative intensity decreases with higher total-oxygen coverage, as is also shown for the precursor in the present work (see next section). Two possible interpretations for the observed losses are discussed in both references. The value of 1230 cm^{-1} is close to the vibrational loss of a double-bonded Si=O molecule, but can also be attributed to the O—O stretching frequency of molecular oxygen with a weakened O—O bond.

Schell-Sorokin and Demuth⁵ exclude molecular oxygen as an interpretation of the 1230 cm^{-1} loss but prefer the Si=O model. The Si=O molecule should be weakly bound to the substrate similar to CO on metals. This model is in disagreement with the aforementioned NEXAFS and XAES results, as is discussed in detail in Ref. 34, in particular because it would involve a molecular axis perpendicular to the surface. Moreover, for a molecule with an electronic structure similar to CO we expect an Auger fine structure which is different from that observed. Finally such a model is not compatible with the present UPS results. The binding energy of peak 3, which would correspond to the CO 1π orbital, is by far lower than expected for Si=O.

In fact, molecular oxygen was excluded by Schell-Sorokin and Demuth⁵ as an explanation for the 1230 cm^{-1} loss because their UP spectra did *not* show pronounced structures at binding energies below 6 eV. However, their spectra taken with unpolarized He I light are similar to ours except for peak 3 [compare our Figs. 5, 7, and 11(b), and Fig. 9 in Ref. 5]. However, they do show weak intensity in the region of peak 5 like our spectra taken with unpolarized He I light [Fig. 11(b)]. Since peak 3 cannot be resolved with poor angular resolution or off-normal emission (cf. Fig. 7), we conclude that Schell-Sorokin and Demuth could not detect the features at low binding energy, and hence the molecular state, due to their accidental choice of experimental parameters.

Ibach *et al.*² preferred a molecular peroxy species as an explanation, in agreement with the present results. The value of 1230 cm^{-1} can be attributed to the O—O stretching frequency of a molecular oxygen adsorbate and is in remarkable agreement with the O—O bond length derived from NEXAFS. Table I compares the results of O₂/Si(111) (Refs. 2, 5, and 34) with those obtained for free O₂ and dioxygen-metal complexes. According to

Vaska, dioxygen-metal complexes can be divided into two classes: superoxo (designated O₂⁻) and peroxy (O₂²⁻) complexes.⁴¹ In both cases the oxygen molecule is *covalently* bound to a (transition) metal, but either one or two electrons have formally been transferred to the antibonding π^* orbital of the O₂ unit. Table I shows that both the O-O distance and the stretching frequency of the precursor are very close to the values of superoxo-metal complexes.

In analogy to the dioxygen-metal complexes we understand the differences of the precursor compared to the isolated O₂ molecule as a change of the electronic structure (rehybridization) of the adsorbed molecule which is accompanied by a charge transfer from the substrate into the antibonding π^* orbital and a reduction of the bond order. These changes weaken the O—O bond and hence reduce the vibrational frequency and increase the bond length. The charge transfer from the substrate to the molecular adsorbate also explains the enormous work-function change $\Delta\Phi$ (Sec. IV B) and the low XPS O 1s binding energy of the precursor (Sec. III D).

In Table I we also include values for the O—O bond lengths and the stretching frequencies for molecular O₂ adsorbates on Pt(111) (Refs. 42–45) and on Ag(110) (Refs. 45–47). Similar to O₂/Si(111) both adsorption systems show oxygen-derived UPS peaks below 8 eV binding energy,^{33,42,48–50} rather low XPS binding energies of the O 1s level [Pt, 530.6 eV (Ref. 31); Ag, 529.6 eV (Ref. 33)], and large work-function changes [Pt, +0.8 eV (Ref. 42); Ag, +0.5–0.7 eV (Ref. 33)]. These data also fit very well to the present results and corroborate our interpretation for the metastable precursor on Si(111).

TABLE I. Bond lengths, O—O stretching frequencies, and bond orders of isolated O₂, superoxo- (O₂⁻) and peroxy- (O₂²⁻) metal complexes, and molecular O₂ adsorbates on Si(111), Pt(111), and Ag(110). Numbers were taken from the references given.

	O—O bond length (Å)	Stretching frequency (cm^{-1})	Bond order
O ₂ gas	1.21 ^a	1580 ^a	2.0
(O ₂ ⁻)	1.31 ^a	1125 ^a	1.5
(O ₂ ²⁻)	1.45 ^a	860 ^a	1.0
O ₂ /Si(111)	1.28 ^{b,c}	1230 ^f	~ 1.5
O ₂ /Pt(111)	1.32 ^{d,e}	870 ^{g,h}	1–1.5
O ₂ /Ag(110)	1.47 ^c	640 ^{i,j}	≤ 1.0

^aReference 41.

^bThis value is based on the evaluation procedure of Ref. 45, but is increased to 1.39 Å if the procedure of Ref. 44 is being used.

^cReference 34.

^dThe result of Ref. 45 differs from that of a previous publication [1.45 Å (Ref. 44)] but appears to be more likely.

^eReference 45.

^fReference 2.

^gReference 42.

^hReference 43.

ⁱReference 46.

^jReference 47.

E. Discussion of the bonding configuration

The present results unambiguously prove that the metastable precursor is a chemisorbed molecular oxygen species. The main arguments for its molecular nature are (a) the additional O 1s peak at 530.6 eV, (b) the additional main UPS peaks at 2.1 and 3.9 eV, which appear in an energy region where no peaks from dissociated oxygen are expected by theory or have been found experimentally, (c) the molecular σ shape resonance,³⁴ (d) the additional Auger peaks, which are only compatible with peaks from a molecular species,³⁴ and (e) the π and σ resonances of the NEXAFS data which are similar to those for O₂/Pt(111) and isolated O₂.³⁴ In the following we concentrate on the discussion of two different bonding configurations, the end-on bonded peroxy radical and the bridge-bonded peroxy molecule. Though, in chemical notation, they should be called "superoxo" according to the NEXAFS and EELS results and Ref. 41, we retain the notations "peroxy radical" and "peroxy bridge" for the O₂ molecule attached to the surface by one and two oxygen atoms, respectively, as this is the tradition in reports on the oxygen interaction with silicon surfaces.

Originally a bridge-bonded oxygen molecule was already proposed by Green and Liberman in 1962 to explain the kinetics of oxygen uptake on silicon and germanium surfaces as observed by gas volumetry.⁵¹ The peroxylike molecule was suggested to be chemisorbed to the Si surface via two dangling bonds. Later Goddard *et al.* proposed the peroxy radical instead.³⁵ It was argued that the O orbitals needed for the surface chemical bond are rotated by 90° for the two atoms and therefore only one O atom should be bonded to the Si surface. However, as the chemisorption of a molecule often leads to a considerable rearrangement of orbitals, geometrical restrictions derived from the isolated molecule need not hold for an adsorbate. Calculations of Bhandia and Schwarz⁵² showed that the chemisorption of a peroxy bridge is energetically possible even on an unreconstructed Si(111) surface with unsaturated dangling bonds rigidly oriented perpendicular to the surface. Thus it does not appear to be justified to rule out one of these models for other than spectroscopic reasons.

There are some observations which make it tempting to identify the precursor with a peroxy radical. First, the O—O distance, the stretching frequency, and the presence of a π resonance in the NEXAFS spectra indicate that the oxygen molecule retains considerable π bonding upon adsorption. This is necessarily the case for the radical configuration. In fact, more superoxo-metal complexes are known with an end-on rather than with a bridge bonding. Second, it is easy to imagine suitable adsorption sites for an end-on bound peroxy radical on the [7×7] reconstructed Si(111) surface, whereas this complicated surface structure does not seem to provide two bonds for a bridging oxygen molecule, at first glance. There are, however, severe arguments against the peroxy radical and in favor of a bridge-bonded molecule which are derived from the NEXAFS, XAES, XPS, and UPS results.

One argument against the peroxy radical arises from the orientation of the molecular axis. While the peroxy

bridge model involves an O—O axis parallel to the surface, in case of the peroxy radical this axis is tilted at least by 26° with respect to the surface plane.⁵³ This tilt should lead to considerable intensity of the σ shape resonance in the NEXAFS spectra taken with the *E* vector perpendicular to the surface plane, and also to a distinct peak from the $\sigma\sigma$ transition in the Auger spectrum, none of which is seen.

Furthermore, the peroxy radical consists of two inequivalent oxygen atoms, which is in disagreement with our XPS results. The spectra of the mixed layers containing the precursor show one rather narrow O 1s peak at 530.6 eV binding energy (compare Fig. 1), while a split of 1.3 eV derived from calculations is expected for the peroxy radical.⁵³ The only alternative explanation would be that the second O 1s peak accidentally coincides with the main O 1s peak from the stable dissociated state. This is not only unlikely, but can also be excluded for quantitative reasons. Such an explanation would require that the major peak at 531.6 eV (Fig. 1) contains a fraction of the precursor which must be equal in intensity to the peak at 530.6 eV. Thus the ratio of molecular to dissociated oxygen would be 2:1 in the mixed layer after 2.5 L oxygen exposure and not 1:2 as derived above. The ratio of 2:1, however, is in disagreement with the corresponding UPS results (cf. Figs. 4 and 5). Peaks 7 and 8, which are due to nonbonding O π -derived orbitals of the stable state, only show a 50%, and not a 150%, increase after annealing of the mixed layer.

Finally, the observed polarization dependence of the UPS peaks disagrees with calculations for the peroxy radical, whereas the peroxy-bridge model allows a straightforward identification of the UPS structures. This is shown in Fig. 9 which compares polarization-dependent He I spectra of a mixed layer with calculated oxygen local density of states (LDOS) for different models taken from different references. At the top, two calculations for dissociated oxygen are displayed.^{36,54} They show that the model for oxygen atoms in bridge positions very well explains energy position and symmetry of peaks 7–9 of the stable state. The calculation for dissociated oxygen in an on-top site is neither compatible with the peak positions and symmetries of the stable state nor with the features from the precursor. This is discussed in detail in part I.¹

Calculations for molecular species are shown in the lower part of Fig. 9. The binding energy scale refers to the Fermi level of our experiment but is adjusted for some of the calculations. (For details on the alignment of scales see figure caption.) From symmetry selection rules applied to atomic $p_{x,y,z}$ states and to $a_1, b_{1,2}$ states of a lying molecule with C_{2v} symmetry we derive for normal emission: states with p_y (in contrast to common assignment, the *y* axis is along the surface normal in these calculations whereas the *z* axis is oriented along the molecular axis) or the a_1 character cannot be excited by radiation with the *E* vector in the surface plane (*s* polarization), but are expected to be predominantly observable for *p* polarization. The opposite is true for $p_{x,z}$ and $b_{1,2}$ derived states, for which we ignore different orientations relative to the surface lattice since various azimuthal orientations of the molecular axis are possible on Si(111).

C_{2v} states are not observable at any polarization in this geometry.

Figure 9 shows that both calculations for the peroxy radical give a symmetry for the topmost levels which is not compatible with the polarization dependence of our peaks 3 and 5. Chen *et al.*,³⁶ who neglect the tilt of the O—O axis, predict two states at 3 and 4 eV binding energy (BE) which must be compared with peaks 3 and 5. Whereas the first peak with O $p_{x,y}$ character should be visible for both polarization directions, the peak at higher BE with O p_z character should be reduced with p polarization in contrast to observation. Goddard *et al.*³⁵ predict higher ionization potentials for the topmost levels

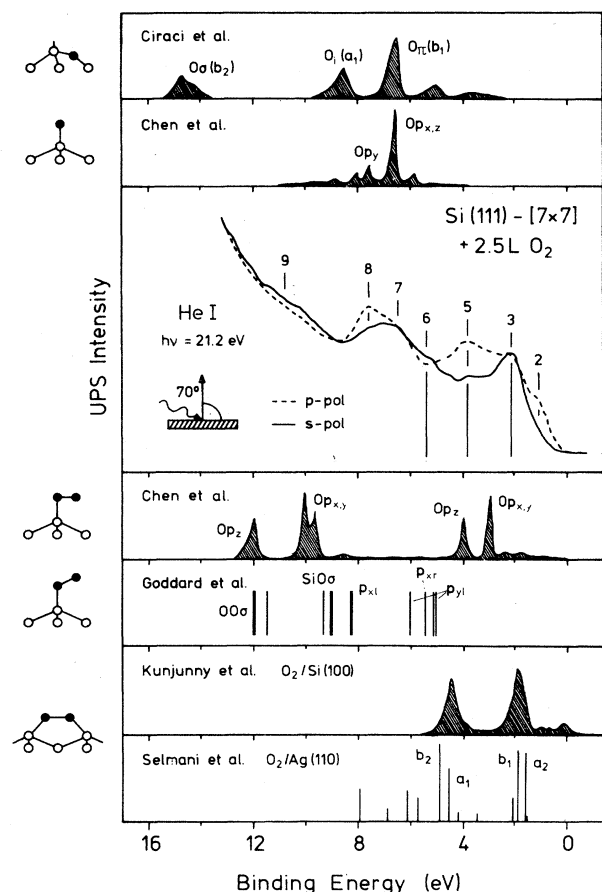


FIG. 9. Comparison of our polarization-dependent He I UPS data from the mixed layer with various calculated oxygen local density of states (LDOS). The calculations are taken from different references and comprise different adsorbate configurations. Atom in short bridge, Ciraci *et al.* (Ref. 54); atom on top, Chen *et al.* (Ref. 36); molecular peroxy radical, Chen *et al.* (Ref. 36); molecular peroxy radical, Goddard *et al.* (Ref. 35) (only ionization potentials); molecular peroxy bridge on Si(100), Kunjunny and Ferry (Ref. 37); molecular peroxy bridge on Ag(110), Selmani *et al.* (Ref. 38). Some of the calculated spectra have been shifted for better alignment by 1.3 eV (Ref. 54) and 0.8 eV (Ref. 36), respectively. Note that the z axis is aligned along the molecular axis, and the y axis represents the surface normal.

than Chen *et al.* Only a complete rearrangement of their energy levels would reproduce the observed polarization dependence in our spectra. Qualitatively this disagreement between calculation and experiment may be understood as follows. In the case of the peroxy radical, $O_2 \pi_g$ -derived electrons are located at the dangling oxygen atom and hence cannot participate in a surface bond. This lone pair should have low binding energy like peak 3, but as it is oriented approximately normal to the surface, it should show a polarization dependence opposite to that observed. In the bridge configuration, however, both oxygen atoms are bound to Si atoms and no lone pair with pure p_y character can be expected.

Regrettably we do not know of any calculation for a peroxy bridge on Si(111). Kunjunny and Ferry who considered $O_2/Si(100)$ do not give symmetries for their LDOS peaks. Thus we can only state that their predicted energy positions are in good agreement with our experimental results.³⁷ We can, however, take the calculations of Selmani *et al.* for $O_2/Ag(110)$ as a basis for a comparison,³⁸ though in this case the O—O bond appears to be considerably weaker as compared to $O_2/Si(111)$. The calculations by Selmani *et al.* for a long bridge site and the shortest considered O—O distance (1.50 Å) show rather good agreement with our results. Peak 5 can be assigned to a π_u -derived a_1 state that disappears for s polarization and shows the molecular σ -like shape resonance. Peak 3 is likely to be due to the $O_2 \pi_g$ -derived b_1 orbital, and peak 6 can be identified with the b_2 orbital. The latter peak, which is not very pronounced in Fig. 9, is clearly discernible with unpolarized He I light, due to better statistics [see, e.g., Fig. 11(b), next section].

Of course, only a detailed calculation for O_2 on Si(111) can confirm the above peak assignment for the bridge-bonded molecule. However, since it is the only configuration that is compatible with all spectroscopic information, we strongly favor it as a model for the precursor. The question of the possible adsorption sites in case of the Si(111)-[7×7] surface will be addressed in the next section.

V. TWO-STAGE ADSORPTION MODEL FOR OXYGEN ADSORPTION ON Si(111)

In part I,¹ the stable oxygen species was characterized as dissociated oxygen, bridge bonded between the first and second Si layer, involving a breaking of Si—Si bonds. Obviously this configuration can be most easily reached through a bridge-bonded peroxylike molecule as intermediate state (Fig. 10). The oxygen molecule first attaches to the dangling bonds of two silicon atoms in the first layer thereby weakening the intramolecular oxygen bond. Thermal or electronic activation then causes the oxygen atoms to flip from the molecular peroxy bond into backbonds between the (initially) involved Si atoms in the first and adjacent Si atoms in the second layer. This model is confirmed by the following results on the coverage dependence of the precursor (V A) and by the results obtained on differently prepared surfaces (V B). Taking into account the metastable nature of the chemisorbed molecule, the various aspects of oxygen uptake on Si(111)

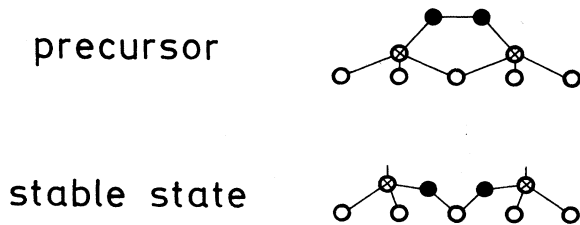


FIG. 10. Suggested model for oxygen adsorption on Si(111) involving precursor and stable state. The positions of silicon (open circles) and oxygen atoms (solid circles) are given for an unreconstructed surface. Possible adsorption sites in the DAS model of the $[7\times 7]$ reconstruction are discussed later in the text.

surfaces are consistently explained by a two-stage adsorption model (V C).

A. Coverage dependence of the precursor

All spectra presented in the last section were taken after an oxygen exposure of 2.5 L yielding a 1:2 ratio of molecular precursor to stable dissociated state. It was not possible to prepare layers consisting of molecular oxygen only, even at substrate temperatures as low as 50 K. Lower coverages, e.g., after exposures of 0.5–1 L oxygen, lead to signals at the limits of a reasonable XPS experiment because the sensibility of the precursor to x-ray radiation requires short recording times (< 10 min). Even at these low coverages dissociated oxygen contributes more than 50% to the total coverage.

The results of Silvestre and Shayegan²⁷ upon adsorp-

tion at 17 K, however, indicate that it is possible to achieve higher coverages of molecular oxygen under certain conditions. The enormous work-function increase of 1.6 eV reported in Ref. 27, which was found after heating to $T > 40$ K to desorb physisorbed oxygen, is a clear evidence for a higher molecular coverage. At higher surface temperatures the $\Delta\Phi$ of Ref. 27 comes close to our values. In Sec. V C we suggest that some coadsorbed dissociated oxygen is necessary to stabilize the precursor on the $[7\times 7]$ reconstructed surface. Before we discuss this idea we should also present the results obtained for different oxygen coverages and for differently prepared surfaces. These results reveal the critical role of the dangling bonds and of the surface reconstruction for the stability of the precursor and for the adsorption kinetics.

Selected results from our experiments on the coverage dependence are collected in Figs. 11(a)–11(c). Figure 11(a) displays the XPS O 1s core spectra which were obtained after different oxygen doses as indicated. With increasing total oxygen coverage the *relative* coverage of the precursor (peak at 530.5 eV) stays approximately constant up to an exposure of 5 L. For higher exposures the absolute coverage of dissociated oxygen increases at a slower rate while that of the precursor stays constant. The resulting uptake curves for the molecular precursor and for the total oxygen coverage are plotted in Fig. 12. The total coverages have been derived by the calibration procedure discussed in part I.¹ Note that the solid curves belong to a substrate temperature of 150 K. At room temperature (dashed line) the initial sticking coefficient (i.e., slope of the curve) is smaller but levels off at higher exposures than at 150 K, thus leading to higher total oxygen coverages after exposures of 10 L and more.

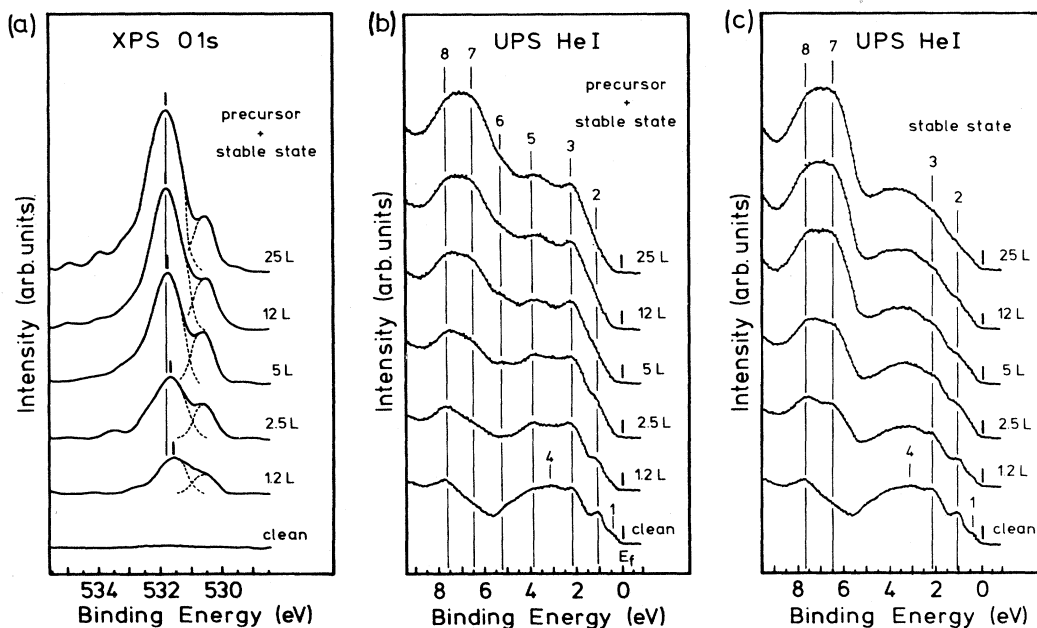


FIG. 11. (a) Series of deconvoluted XPS O 1s spectra obtained immediately after various oxygen exposures at 150 K containing precursor and stable state; (b) UPS He I spectra of the same layers; (c) UPS He I spectra of these layers taken after decay of the molecular precursor upon annealing at 400 K.

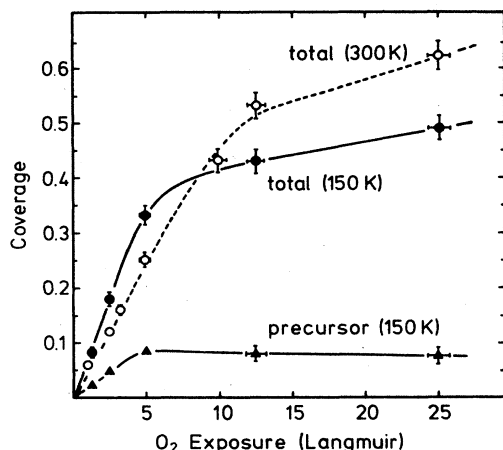


FIG. 12. Oxygen-uptake curves for $O_2/Si(111)-[7 \times 7]$ at 150 and 300 K. For 150 K the total coverage and the contribution of the molecular precursor are shown. The coverage refers to Si surface atoms, $1.12 \times 10^{15} \text{ cm}^{-2}$.

In Figs. 11(b) and 11(c) He I UPS spectra taken before and after annealing at 400 K are shown. They were recorded with unpolarized light at normal emission with an angular resolution of $\pm 1^\circ$. Though the various structures are not as pronounced as they are with polarized light (compare Fig. 5) they can easily be identified and are labeled 1–8 as above. A comparison with the XPS spectra shows a consistent increase of the oxygen-derived structures with coverage. For peak 2 we observe a very interesting behavior. This peak vanishes for saturation of the precursor after an exposure of 5 L [Fig. 11(b)], but some of its intensity reappears after conversion of molecular oxygen into the stable dissociated state by annealing [Fig. 11(c)].

Peak 2 is due to a surface state of the $[7 \times 7]$ reconstructed silicon surface.⁵⁵ On the basis of the dimer–adatom–stacking-fault (DAS) model of the $[7 \times 7]$ reconstruction⁵⁶ Northrup identified this surface state as doubly occupied dangling-bond states located at the six rest atoms of the $[7 \times 7]$ unit cell.⁵⁷ The rest atoms are threefold coordinated surface atoms which are not bonded to an adatom.⁵⁶ The behavior of peak 2 upon adsorption thus indicates that the molecular precursor is chemisorbed to these dangling bonds, while they are less affected by the stable dissociated state, as expected for the model suggested. Peak 1, which is also due to a surface state, shows qualitatively the same behavior. This is best seen in Fig. 11 when the distances between valence-band maximum and E_f are compared in the spectra taken before and after annealing. According to Northrup, this surface state is composed of substrate dangling-bond states and adatom p_z orbitals. This information is needed for the discussion of the adsorption sites in Sec. V C. We note that this assignment of surface states to certain sites within the DAS model is also evident from the scanning tunneling microscope studies by Hamers *et al.*⁵⁸

B. Influence of surface reconstruction

An adsorption mechanism involving the dangling bonds should depend on surface reconstruction. In Fig.

13 we show He I UPS spectra of differently prepared Si(111) surfaces of two samples *a* and *b*. Though cut from the same wafer, spectra from the two clean $[7 \times 7]$ reconstructed surfaces show some differences. Sample *b* which exhibited the sharper $[7 \times 7]$ LEED pattern also yielded sharper UPS peaks from the characteristic $[7 \times 7]$ surface states 1 and 2. The differences might be caused by different quality of the polishing procedure or by contamination. Although the spectrum of sample *a* does show some similarity to the carbon-contaminated sample *b*, as seen in Fig. 13, we can exclude this possibility because all samples have been regularly monitored for carbon contamination with XPS. Instead, we suspect that the doping material phosphorus could be enriched at the surface in the case of sample *a*. The XPS P 3*p* peaks are in the same energy range as the strong plasmon losses of Si 2*p*, and hence small amounts of phosphorus cannot be distinguished. The surface enrichment of a constituent may be caused by the annealing of the crystal to light redheat for several hundred times. In the case of a heavily boron-doped sample a similar effect has been reported very recently.⁵⁹

Qualitatively all $[7 \times 7]$ surfaces showed the same spectral features after oxygen adsorption. The reactivity was highest for the clean sample *b*. The total oxygen coverage after a 2.5 L dose was smaller by 30% in the case of sample *a* and by 20% in the case of the heavily carbon-contaminated surface *b*. No significant difference could be observed comparing the clean and the weakly carbon contaminated surface. The *relative* amount of molecular

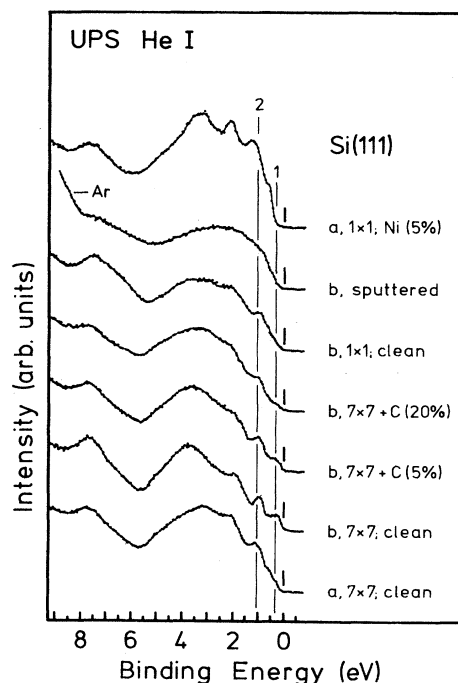


FIG. 13. He I valence-band spectra of differently prepared, clean Si(111) surfaces. *a* and *b* indicate two different samples. The carbon and nickel contamination in the surface region was determined by XPS and is given in percent with respect to Si surface atoms ($1.12 \times 10^{15} \text{ cm}^{-2}$).

oxygen was the same for all $[7 \times 7]$ surfaces within the experimental error of $< 10\%$.

Marked differences were observed between the differently prepared clean surfaces. In the upper part of Fig. 13 three spectra are compared which show the valence bands of a sputtered and slightly annealed surface (labeled $[1 \times 1]$; clean), an Ar-sputtered, nonannealed surface, and a quasi- $[1 \times 1]$ surface, stabilized by 0.05 ML Ni after heating to about 1100 K,¹¹ that did not show an overstructure in the LEED pattern. Figure 14 displays the corresponding He II spectra obtained after an oxygen exposure of 2.5 L at 300 K. The intensity of peak 5 identifying the precursor decreases when comparing the $[7 \times 7]$ reconstructed, the sputter-annealed, and finally the $[1 \times 1]$ Ni surface. It is correlated with the decreasing intensity of the dangling-bond peak 2 (Fig. 13). Figures 7, 9, and 10 of part I (Ref. 1) complement this finding in the coverage range from 2.5 to 250 L O_2 .

C. Fast and slow stages of oxygen adsorption

The observed coverage dependence and the influence of surface preparation suggest the following: As long as the Si surface provides free dangling bonds and adsorption sites, molecular oxygen can be chemisorbed, leading to a relatively high sticking coefficient. Once chemisorbed, the peroxy molecule can dissociate, and oxygen atoms are inserted into the backbonds of the top Si layer. If suitable bonds for attachment of molecular oxygen are exhausted the oxygen molecules must dissociate and break the backbonds in a different way in order to be adsorbed. Since this is probably a more complicated and thus less likely process it leads to a lower sticking coefficient.

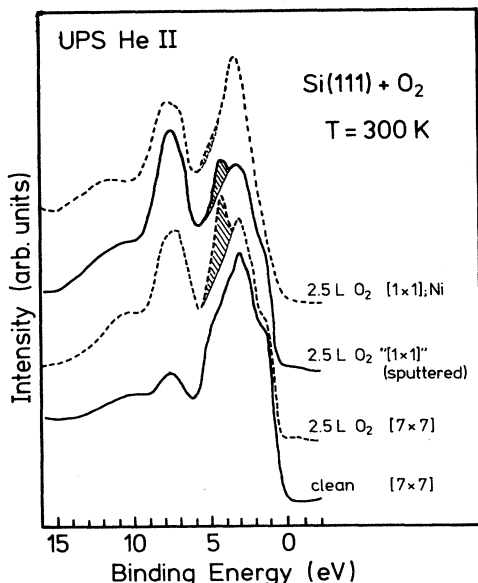


FIG. 14. He II UP spectra taken immediately after exposure of differently prepared Si(111) surfaces to 2.5 L oxygen at room temperature. The hatched area indicates the varying contribution of the molecular precursor (peak 5 in Figs. 5–7). The sputtered $[1 \times 1]$ surface was obtained by sputtering and slight annealing to remove implanted Ar.

The proposed two-stage adsorption model involving the molecular precursor easily explains various kinetic aspects of oxygen adsorption under different conditions. The first measurements using gas volumetry already showed that a fast initial-adsorption stage is followed by a slower sorption process.⁶⁰ As, for example, seen in the uptake curve of Fig. 12 in part I,¹ the sticking coefficient drops for the Si(111)- $[7 \times 7]$ surface by a factor of 10 between 10 and 25 L though the total oxygen coverage is still well below a monolayer. Up to this exposure (10–25 L) we always found significant precursor peaks in the UP spectra (compare, e.g., Fig. 7, part I).

The differences between the uptake curves obtained at 150 and 300 K (Fig. 12), respectively, are also a direct consequence of the precursor and its decay. At low substrate temperatures the decay rate is slow compared to the dosing time. The consequence is that most of the available dangling bonds are saturated by molecular oxygen at relatively low coverages leading to a drop of the sticking coefficient between 5 and 10 L exposure. Thus for doses higher than 10 L the total coverage at 150 K is smaller than that at 300 K, despite the higher initial sticking probability.

A sputtered and slightly annealed surface shows a $[1 \times 1]$ LEED pattern and is likely to be recrystallized in the topmost layer, with some sputter-induced amorphous Si layers underneath. This idea has been proposed by Comin *et al.*⁶¹ based on surface extended x-ray-absorption fine structure (SEXAFS) measurements. It is corroborated by our present UPS data (Fig. 13) which show significant emission from the surface states 1 and 2. The observation of these states also suggests that the adsorption behavior on this surface should be similar to that on the clean $[7 \times 7]$ surface, but eventually involving less molecular oxygen. This is indeed observed if we compare, for instance, the coverage dependence of peak 5 in the UPS spectra of Figs. 7 and 9 in part I.¹ Moreover the fast-adsorption stage ends at lower total coverage (already below 10 L on the $[1 \times 1]$ surface) leading to a lower overall sticking coefficient (compare Fig. 12, part I). The results from the sputtered and sputter-annealed surfaces also exclude the possibility that the observed molecular precursor is a minority species bound to defects on the surface, as one might be tempted to suspect from the low coverages.

In the case of the $[1 \times 1]$ Ni surface we did not see features of the precursor. We suspect that mainly a different arrangement and orientation (or a lack) of dangling bonds, and not the presence of metallic sites, lead to the lower sticking probability and to the shorter lifetime of the precursor on this surface. We also observed a lower absolute sticking coefficient and a more gradual change with exposure than on the $[7 \times 7]$ surface as expected from our model.

Finally we discuss possible adsorption sites for the precursor on the $[7 \times 7]$ reconstructed surface. As described by the DAS model, the number of terminating silicon atoms that are only threefold coordinated is drastically reduced upon reconstruction compared to a truncated (111) surface. Only the 12 adatoms, the six rest atoms, and the corner atom of the $[7 \times 7]$ unit cell are reasonable

candidates for an attachment of oxygen molecules in view of the above discussion. The corner atom may be involved but it cannot account for the entire amount of adsorbed molecular oxygen. The distance between two adatoms, or even two rest atoms is very large compared to the O—O bond length of 1.3 Å and the normally observed Si—O bond lengths of about 1.6 Å. Only the distance of about 4 Å between a rest atom and a neighboring adatom is accessible for a bridging oxygen molecule on the undisturbed [7×7] surface. These adsorption sites are in agreement with the observed effect on the dangling-bond states 1 and 2.

However, we do not believe that we mainly observe this configuration in our measurements. This adsorbate configuration is likely to be rather unstable and to dissociate quickly leading to bridge-bonded atomic oxygen. Dissociated oxygen then leads to a rearrangement of the surface, especially in the layer of the adatoms. Now suitable adsorption sites may exist in the layer of the rest atoms. The oxygen molecule can then be bonded with one end to a rest atom and with the other end to an atom previously attached to an adatom. Such sites should have a similar geometry as that sketched in Fig. 10. Since the involved silicon atoms are rather tightly bound in this configuration, a relatively long lifetime of the precursor is plausible.

Of course, some of these last ideas are still somewhat speculative at the moment. More experiments and especially calculations for different adsorbate geometries that can be compared to the present data set could help to get more insight. We believe that our model of oxygen adsorption involving a molecularly chemisorbed precursor is also applicable to other silicon surfaces and perhaps to other semiconductor surfaces. Very recently published results on the Si(110) surface support this suggestion.¹²

VI. SUMMARY

The initial stage of oxygen adsorption on Si(111) involves two different adsorbate configurations: a stable

dissociated oxygen species and a molecularly chemisorbed precursor.

Using high-resolution XPS, work-function data, and polarization-dependent UPS we have characterized the precursor as a superoxolike bridging molecule attached to the surface via two dangling bonds. This interpretation is supported by high-resolution XAES, NEXAFS,³⁴ and HREELS^{2,5} results published elsewhere. The stable state is an oxygen atom in bridge position between silicon atoms in the first and second layer, as described in part I.¹

The decay of the precursor and its conversion to the stable state could be monitored by XPS on the Si(111)-[7×7] surface, for which the lifetime of the precursor was found to be highest. The decay is a thermally or electronically activated process. We estimate a thermal activation energy of 0.24 eV on the [7×7] surface.

On the basis of the suggested two-stage adsorption model involving the molecular precursor, it is possible to explain the dependence of the sticking coefficient upon exposure, temperature, and surface preparation. The observed decrease of the sticking coefficient by one order of magnitude in the submonolayer regime is understood as an exhaustion of suitable sites for the adsorption of molecular oxygen.

ACKNOWLEDGMENTS

We would like to express our gratitude to Professor D. Menzel for general support and helpful discussions. We further thank A. Puschmann and D. Coulman for their contributions to the synchrotron-radiation experiments, E. Hudeczek and H. Eichele for technical help, P. Feulner for valuable discussions, and G. Höfer for drawing the figures. This project was financially supported by the Deutsche Forschungsgemeinschaft through Sonderforschungsbereich 128, by the German Ministry of Research and Technology under Grant No. 05-366-CAB, and by Odense University, Odense, Denmark.

*Permanent address: Fysisk Institut, Odense Universitet, Campusvej 55, DK-5230 Odense M, Denmark.

¹P. Morgen, U. Höfer, W. Wurth, and E. Umbach, *Phys. Rev. B* **39**, 3720 (1989).

²H. Ibach, H. D. Bruchmann, and H. Wagner, *Appl. Phys.* **A29**, 113 (1982).

³G. Hollinger and F. J. Himpsel, *Phys. Rev. B* **28**, 3651 (1983); *J. Vac. Sci. Technol. A* **1**, 640 (1983).

⁴U. Höfer, P. Morgen, W. Wurth, and E. Umbach, *Phys. Rev. Lett.* **55**, 2979 (1985).

⁵A. J. Schell-Sorokin and J. E. Demuth, *Surf. Sci.* **157**, 273 (1985).

⁶G. Hollinger, J. F. Morar, F. J. Himpsel, G. Hughes, and J. L. Jordan, *Surf. Sci.* **168**, 609 (1986).

⁷G. Hollinger and F. J. Himpsel, *Appl. Phys. Lett.* **44**, 93 (1984).

⁸P. J. Grunthaner, M. H. Hecht, F. J. Grunthaner, and N. M. Johnson, *J. Appl. Phys.* **61**, 629 (1987).

⁹W. Braun and H. Kuhlbeck, *Surf. Sci.* **180**, 279 (1987).

¹⁰A. Franciosi, P. Soukiasian, P. Philip, S. Chang, A. Wall, A. Raisanen, and N. Troullier, *Phys. Rev. B* **35**, 910 (1987).

¹¹P. Morgen, W. Wurth, and E. Umbach, *Surf. Sci.* **153**, 1086 (1985).

¹²E. G. Keim and A. van Silfout, *Surf. Sci.* **186**, L557 (1987); E. G. Keim, A. van Silfout, and L. Wolterbeek, *J. Vac. Sci. Technol. A* **6**, 57 (1988).

¹³Z. Ying and W. Ho, *Phys. Rev. Lett.* **60**, 57 (1988).

¹⁴E. G. Keim, L. Wolterbeek, and A. van Silfout, *Surf. Sci.* **180**, 565 (1987).

¹⁵K. Uno, A. Namiki, S. Zaima, T. Nakamura, and N. Ohtake, *Surf. Sci.* **193**, 321 (1988).

¹⁶C. M. Garner, I. Lindau, C. Y. Su, P. Pianetta, J. N. Miller, and W. E. Spicer, *Phys. Rev. Lett.* **40**, 403 (1978); *Phys. Rev. B* **19**, 3944 (1979).

¹⁷U. Höfer, Diplomarbeit, Technical University München, 1985; U. Höfer and E. Umbach (unpublished).

¹⁸S. Haykin and S. Kessler, in *Nonlinear Methods of Spectral Analysis*, edited by S. Haykin (Springer, Berlin, 1979).

¹⁹E. L. Kosarev and E. Pantos, *J. Phys. E* **16**, 537 (1983).

²⁰W. H. Press, B. P. Flannery, S. A. Teukolsky, and W. T. Vetterling, *Numerical Recipes, The Art of Scientific Comput-*

- ing (Cambridge University Press, Cambridge, 1986).
- ²¹P. Hofmann, J. Gossler, A. Zartner, M. Glanz, and D. Menzel, *Surf. Sci.* **61**, 303 (1985); G. Michalk and D. Menzel (unpublished).
- ²²A. F. Carley and R. W. Joyner, *J. Electron. Spectrosc.* **16**, 1 (1979).
- ²³P. A. Jansson, R. H. Hunt, and E. K. Plyler, *J. Opt. Soc. Am.* **60**, 596 (1970).
- ²⁴B. R. Frieden, in *Picture Processing and Digital Filtering*, edited by T. S. Huang (Springer, Berlin, 1979).
- ²⁵R. P. Vaquez, J. D. Klein, J. J. Barton, and F. J. Grunthaler, *J. Electron. Spectrosc.* **23**, 63 (1981).
- ²⁶U. Gelius, L. Asplund, E. Basilier, S. Hedman, K. Helensund, and K. Siegbahn, *Nucl. Instrum. Methods B* **1**, 85 (1984).
- ²⁷C. Silvestre and M. Shayegan, *Phys. Rev. B* **37**, 10432 (1988).
- ²⁸*Practicle Surface Analysis*, edited by D. Briggs and M. P. Seah (Wiley, Chichester, 1983).
- ²⁹D. Menzel, *Nucl. Instrum. Methods B* **13**, 507 (1986).
- ³⁰M. Pedio, J. C. Fuggle, J. Somers, E. Umbach, J. Haase, Th. Lindner, U. Höfer, M. Grioni, F. de Groot, B. Hillert, L. Becker, and A. Robinson (unpublished).
- ³¹G. B. Fisher, B. A. Sexton, and J. L. Gland, *J. Vac. Sci. Technol.* **17**, 144 (1980).
- ³²W. Ranke and H. J. Kuhr, *Phys. Rev. B* **39**, 1595 (1989).
- ³³J. Eickmans, A. Otto, and A. Goldmann, *Surf. Sci.* **149**, 293 (1985).
- ³⁴U. Höfer, A. Puschmann, D. Coulman, and E. Umbach, *Surf. Sci.* **211/212**, 948 (1989).
- ³⁵W. A. Goddard, III, A. Redondo, and T. C. McGill, *Solid State Commun.* **18**, 981 (1976).
- ³⁶M. Chen, I. P. Batra, and C. R. Brundle, *J. Vac. Sci. Technol.* **16**, 1216 (1979).
- ³⁷T. Kunjunny and D. K. Ferry, *Phys. Rev. B* **24**, 4593 (1981).
- ³⁸A. Selmani, J. M. Sichel, and D. R. Salahub, *Surf. Sci.* **157**, 208 (1985).
- ³⁹K. Siegbahn, C. Nordling, G. Johansson, J. Hedman, P. F. Heden, K. Hamrin, U. Gelius, T. Bergmark, L. O. Werme, R. Manne, and Y. Baer, *ESCA Applied to Free Molecules* (North-Holland, Amsterdam, 1971).
- ⁴⁰L. S. Cederbaum, W. Domcke, J. Schirmer, and W. von Niessen, in *Advances in Chemical Physics*, edited by I. Prigogine and S. A. Rice (Wiley, New York, 1986), Vol. 65, p. 115.
- ⁴¹L. Vaska, *Acc. Chem. Res.* **9**, 175 (1976).
- ⁴²J. L. Gland, B. A. Sexton, and G. B. Fisher, *Surf. Sci.* **95**, 587 (1980).
- ⁴³H. Steininger, S. Lehwald, and H. Ibach, *Surf. Sci.* **123**, 1 (1982).
- ⁴⁴J. Stöhr, J. L. Gland, W. Eberhardt, D. Outka, R. J. Madix, F. Sette, R. J. Koestner, and U. Doebler, *Phys. Rev. Lett.* **51**, 2414 (1983).
- ⁴⁵D. A. Outka, J. Stöhr, W. Jark, P. Stevens, J. Solomon, and R. J. Madix, *Phys. Rev. B* **35**, 4119 (1987).
- ⁴⁶B. A. Sexton and R. J. Madix, *Chem. Phys. Lett.* **76**, 294 (1980).
- ⁴⁷C. Backx, C. P. M. de Groot, and P. Biloen, *Surf. Sci.* **104**, 300 (1981).
- ⁴⁸K. C. Prince and A. M. Bradshaw, *Surf. Sci.* **126**, 49 (1983).
- ⁴⁹M. A. Barteau and R. J. Madix, *Chem. Phys. Lett.* **97**, 49 (1983).
- ⁵⁰K. C. Prince, G. Paolucci, and A. M. Bradshaw, *Surf. Sci.* **175**, 101 (1986).
- ⁵¹M. Green and A. Liberman, *J. Phys. Chem. Solids* **23**, 1407 (1962).
- ⁵²A. S. Bhandia and J. A. Schwarz, *Surf. Sci.* **108**, 587 (1981).
- ⁵³A. Redondo, W. A. Goddard, III, C. A. Swarts, and T. C. McGill, *J. Vac. Sci. Technol.* **19**, 498 (1981).
- ⁵⁴S. Ciraci, S. Ellialtioglu, and S. Erkoc, *Phys. Rev. B* **26**, 5716 (1982).
- ⁵⁵R. I. G. Uhrberg, G. V. Hansson, J. M. Nicholls, P. E. S. Persson, and S. A. Flodström, *Phys. Rev. B* **31**, 3805 (1985).
- ⁵⁶K. Takayanagi, Y. Tanishiro, M. Takahashi, and S. Takahashi, *J. Vac. Sci. Technol. A* **3**, 1502 (1985); *Surf. Sci.* **164**, 367 (1985).
- ⁵⁷J. E. Northrup, *Phys. Rev. Lett.* **57**, 154 (1986).
- ⁵⁸R. J. Hamers, R. M. Tromp, and J. E. Demuth, *Phys. Rev. Lett.* **56**, 1972 (1986).
- ⁵⁹F. Thibaudau, Ph. Dumas, Ph. Mathiez, A. Humbert, D. Satti, and F. Salvan, *Surf. Sci.* **211/212**, 148 (1989).
- ⁶⁰J. T. Law, *J. Phys. Chem. Solids* **4**, 91 (1958); M. Green and K. H. Maxwell, *J. Phys. Chem.* **1**, 145 (1960).
- ⁶¹F. Comin, L. Incoccia, P. Lagarde, G. Rossi, and P. H. Citrin, *Phys. Rev. Lett.* **54**, 122 (1985).